New Journal and we have not received input yet 22 (2021) 100817

Contents lists available at ScienceDirect

Thermal Science and Engineering Progress

journal homepage: www.sciencedirect.com/journal/thermal-science-and-engineering-progress

Heat and work fluxes in thermoelectric coolers

Javier Garrido *, José A. Manzanares

Departamento de Termodinámica, Universitat de Valencia, 46100 Burjassot, Valencia, Spain

ARTICLE INFO

Keywords:
Work flux
Work transfer
Thermoelectric cooler
Thomson effect
Peltier effect

ABSTRACT

Thermodynamics considers heat and work as the observables of energy. Then, in a non-equilibrium process, the fluxes of heat, work and energy are related. The expressions for the heat and energy flux densities are well known; although several conventions have been adopted. The work flux density defined from the heat and energy flux densities can be very useful in describing the energy balance when chosen to emphasize observable quantities. This paper discusses the advantages of the use of the conduction heat flux density given by Fourier's law and a work flux density defined from it. As a case study, heat and work fluxes are evaluated in the elements of a thermoelectric cooler using both the observable formalism and the electrochemical formalism. Two components, Thomson and Joule, are distinguished in the work rate of the semiconductors. In the *p*-type leg, absorption due to the Thomson effect of up to 33% of the electric power dissipated by Joule's effect is observed. It is also concluded that the observable voltage drop is proportional to the electrical power consumed in the TEC and in its connectors, but not in the semiconductor legs and in the semiconductor/connector junctions.

1. Introduction

Thermoelectric coolers (TEC) receive electric power and extract heat from a cold source. Thermoelectric generators generate electric power from the heat transfer between the hot source and the cold source. To optimize these modes of operation of thermoelectric modules it is necessary to apply an energy balance. This balance is usually carried out by operating with widely accepted expressions on energy and heat flux densities [1–15]. In this paper the analysis of the energy balance will be developed considering a third flux that measures the electrical power received in the thermoelectric material: the work flux. This new way of approaching the energy balance will question the usual expression of the heat flux.

The first law of thermodynamics evidences that heat Q and work W are the observable quantities of energy, $\Delta U = Q - W$. In a thermoelectric element (TE) the rates of these quantities $\dot{U}$, $\dot{Q}$ and $\dot{W}$ are related to the energy flux density $\boldsymbol{j}_{\mathrm{u}}$, the heat flux density $\boldsymbol{j}_{\mathrm{q}}$, and the work flux density $\boldsymbol{j}_{\mathrm{w}}$. The work flux density is defined as $\boldsymbol{j}_{\mathrm{w}} = \boldsymbol{j}_{\mathrm{q}} - \boldsymbol{j}_{\mathrm{u}}$. The fluxes of heat and energy are often discussed but, to the best of our knowledge, no reference has been made to the work flux in the literature in spite of the fact that it may provide very practical, complementary information in the energy balance.

In thermoelectric processes, as in any other, energy is conserved. This principle, together with a sound phenomenological basis that involves the description of four effects (named after Fourier, Peltier, Joule and Thomson) provides a solid theoretical foundation for the expression of the total energy flux density [1,2]. On the contrary, the expressions for the heat flux density are based on conventions. For example, in the electrochemical formalism [3], the expression $\boldsymbol{q} = \Pi \boldsymbol{i} - \kappa \nabla T$, where Π is the Peltier coefficient and κ the thermal conductivity, is based on its relation with the entropy flux density, $\boldsymbol{q} = T\boldsymbol{j}_{\mathrm{s}}$ [1,2]. The conduction heat flux density given by Fourier's law $\boldsymbol{j}_{\mathrm{q}} = -\kappa \nabla T$ is a more convenient choice to describe observable energy transfers.

These concepts become clear when considering the energy balance in a TEC under typical operating conditions [16]. The calculation of the energy, heat and work fluxes in the different cross-sections of the TEC allows the determination of the heat and work rates in every TE. The comparison of the energy balances using both the electrochemical formalism and the observable formalism evidences the observable character of the heat rates calculated from $\boldsymbol{j}_{\mathrm{q}}$.

The electrical power that a TE receives by Joule effect is always positive, but the electrical power that a TE receives due to the Thomson effect can be negative. In order to illustrate the partial compensation of these two effects, the electrical power consumed by the semiconductor legs in the TEC is evaluated.

Another observable in thermoelectric elements is the voltage. This quantity might measure the power supplies by the electrical current to a TE. Noteworthy, although the electrical power is proportional to the observable voltage drop when considering the whole TEC, this is not the

* Corresponding author.
E-mail address: javier.garrido@uv.es (J. Garrido).

https://doi.org/10.1016/j.tsep.2020.100817
Received 17 August 2020; Received in revised form 14 December 2020; Accepted 16 December 2020

Nomenclature

A	area (m^2)
e	elementary charge (C)
$\boldsymbol{i}$	electric current density (Am^{-2})
I	electric current (A)
$\boldsymbol{j}_q$	observable heat flux density (Wm^{-2})
$\boldsymbol{j}_s$	entropy flux density ($Wm^{-2}K^{-1}$)
$\boldsymbol{j}_u$	energy flux density (Wm^{-2})
$\boldsymbol{j}_w$	observable work flux density (Wm^{-2})
J_q	observable heat flux (W)
J_u	energy flux (W)
J_w	observable work flux (W)
P	electric power (W)
Q	heat (J)
$\dot{Q}$	observable heat rate in a TE (W)
$\left[\dot{Q}\right]$	heat rate in a TE in the electrochemical formalism (W)
$\boldsymbol{q}$	heat flux density in the electrochemical formalism (Wm^{-2})
S	Seebeck coefficient (VK^{-1})
t	time (s)
T	thermodynamic temperature (K)
TE	thermoelectric element
TEC	Thermoelectric cooler
U	internal energy (J)
$\dot{U}$	internal energy rate (W)
V	volume (m^3)
V_Z	voltage measured by probes Z (V)
W	work (J)
$\dot{W}$	observable work rate in a TE (W)
$\left[\dot{W}\right]$	work rate in a TE in the electrochemical formalism (W)
x	position coordinate along the current (m)
Z	metal of the probes for measuring the voltage

Subscripts

c	cold side
con	contact
ext	external source of heat
h	hot side
in	incoming
n	*n*-type semiconductor
out	outgoing
p	*p*-type semiconductor
ref	reference
surr	surroundings
syst	system
I	negative terminal
II	positive terminal

Greek letters

κ	thermal conductivity ($Wm^{-1}K^{-1}$)
μ	electrochemical potential of the electron (J)
Π	Peltier coefficient (V)
ρ	electrical resistivity (Ωm)
τ	Thomson coefficient (VK^{-1})

case when considering the semiconductor legs.

2. Theory

2.1. Observable heat and work rates

In thermoelectricity, the total energy flux density is [1–3,11]

$$\boldsymbol{j}_u = -\kappa\nabla T + \left(\Pi - \frac{\mu}{e}\right)\boldsymbol{i} \tag{1}$$

where κ the thermal conductivity, Π is the Peltier coefficient, μ is the electrochemical potential of the electron, e (>0) is the elementary charge, and $\boldsymbol{i}$ is the electric current density. In the cited references other symbols are used instead of $\boldsymbol{j}_u$ but there is no discussion about the validity of Eq. (1). It is well known in thermodynamics of irreversible processes that different choices of fluxes and driving forces can be used in the formulation of the transport equations, provided that the entropy production rate remains invariant [3]. One of the fluxes regularly used is the electric current density $\boldsymbol{i}$. The other flux is thermal, but there is a some diversity both in the choices and in their denominations. For example, the heat flux density $\boldsymbol{q}$ defined in Ref. [16] is the same as $\boldsymbol{j}_u$ in Eq. (1). Most frequently, the heat flux density is defined as $\boldsymbol{q} = \Pi\boldsymbol{i} - \kappa\nabla T$ [11]. Yet, other definitions are also consistent with the physical principles of irreversible thermodynamics [3], such as the conduction heat flux density $\boldsymbol{j}_q = -\kappa\nabla T$. The definition chosen is ultimately justified by the theoretical formalism used or by a character of the flux that is emphasized.

Work and heat, or their transfer rates, electrical power and cooling/heating capacity are the observables of energy. Since the distinction between these two forms of energy transfer is essential in thermal sciences, the decomposition

$$\boldsymbol{j}_u = \boldsymbol{j}_q - \boldsymbol{j}_w \tag{2}$$

of the energy flux density $\boldsymbol{j}_u$ into a heat flux density and a work flux density should be considered when analyzing the energy conversion in thermoelectric devices. The steady-state, energy balance $\dot{U} = \dot{Q} - \dot{W} = 0$ for a system occupying a domain Ω bounded by the surface $\partial\Omega$ requires that the net energy flux across its boundary must vanish,

$$\dot{U} = -\oiint_{\partial\Omega} \boldsymbol{j}_u \cdot \mathrm{d}\boldsymbol{A} = -\iiint_{\Omega} \nabla\cdot\boldsymbol{j}_u \mathrm{d}V = 0 \tag{3}$$

$$\dot{Q} - \dot{W} = -\oiint_{\partial\Omega} \boldsymbol{j}_q \cdot \mathrm{d}\boldsymbol{A} + \oiint_{\partial\Omega} \boldsymbol{j}_w \cdot \mathrm{d}\boldsymbol{A} = -\iiint_{\Omega} \nabla\cdot\boldsymbol{j}_q \mathrm{d}V + \iiint_{\Omega} \nabla\cdot\boldsymbol{j}_w \mathrm{d}V = 0 \tag{4}$$

where $\mathrm{d}\boldsymbol{A}$ is an oriented surface element. The heat rate and the work rate in a volume element $\mathrm{d}V$ are given by the divergences of the flux densities, $\mathrm{d}\dot{Q} = -\nabla\cdot\boldsymbol{j}_q \mathrm{d}V$ and $\mathrm{d}\dot{W} = -\nabla\cdot\boldsymbol{j}_w \mathrm{d}V$. These quantities are transferred through the boundaries of the volume element.

The heat and work rates, $\dot{Q}$ and $\dot{W}$, observed in a system are also the heat and work rates exchanged between the system and its surroundings,

$$\dot{Q} = \dot{Q}_{\mathrm{surr}\to\mathrm{syst}} \tag{5}$$

$$\dot{W} = \dot{W}_{\mathrm{surr}\to\mathrm{syst}}. \tag{6}$$

Then, the electric power transferred from the surroundings to the system is the negative of the work rate $\dot{W}_{\mathrm{surr}\to\mathrm{syst}}$

$$P_{\mathrm{surr}\to\mathrm{syst}} = -\dot{W}_{\mathrm{surr}\to\mathrm{syst}}. \tag{7}$$

When $\dot{Q} = \dot{W} < 0$, the thermoelectric system receives energy from the surroundings as electrical power and transfers it to the surroundings as heat rate. When $\dot{Q} = \dot{W} > 0$, the system transfers energy to the surroundings as electrical power and receives it as heat rate.

2.2. Heat and work transport equations

Several formulations of the equations of thermoelectricity are in use, each with its advantages and disadvantages [3]. In this work, the transport equations are Eq. (1) and

$$\frac{1}{e}\nabla\mu = S\nabla T + \rho \boldsymbol{i} \tag{8}$$

where S is the Seebeck coefficient and ρ is the electrical resistivity. These equations have a phenomenological basis and adequately describe six effects: Fourier, Peltier, Thomson, Joule, Ohm, and Seebeck [17–20]. The non-equilibrium state is locally determined by ∇T and $\boldsymbol{i}$.

There are also several possibilities to define the flux densities of heat and work in Eq. (2). We consider two of them. The first one, in this paragraph, is preferred because it is the one compatible with the observable character of heat and work. The divergences of the flux densities of heat and work

$$\boldsymbol{j}_{\rm q} = -\kappa\nabla T \tag{9}$$

$$\boldsymbol{j}_{\rm w} = \left(\frac{\mu}{e} - \Pi\right)\boldsymbol{i} \tag{10}$$

must express, respectively, the heat rate and the work rate (or electrical power) in the material. Under steady-state conditions, the charge conservation and energy conservation require

$$\nabla\cdot\boldsymbol{i} = 0 \tag{11}$$

$$\nabla\cdot\boldsymbol{j}_{\rm u} = 0. \tag{12}$$

Then, from Eqs. (1), (8), (11) and (12), the divergences of the heat and work flux densities are

$$\nabla\cdot\boldsymbol{j}_{\rm q} = \nabla\cdot(-\kappa\nabla T) \tag{13}$$

$$\nabla\cdot\boldsymbol{j}_{\rm w} = -\tau\boldsymbol{i}\cdot\nabla T + \rho\boldsymbol{i}^2 \tag{14}$$

where $\tau = {\rm d}\Pi/{\rm d}T - S$ is the Thomson coefficient. Two remarkable features are: i) the transport coefficients κ, τ, and ρ can be measured, and ii) the electrical current density appears in the expression of $\nabla\cdot\boldsymbol{j}_{\rm w}$, but not in $\nabla\cdot\boldsymbol{j}_{\rm q}$, i.e., the electric current is related to the electrical power but not the heat rate.

To further clarify the arguments that support our preference for Eqs. (9) and (10), another possible definition of the work flux density, that corresponds to the electrochemical formalism in thermoelectricity [3], is considered next. Indisputably, the total energy flux density $\boldsymbol{j}_{\rm u}$ must be given by Eq. (1) and the difference between the heat flux density and the work flux density must be equal to $\boldsymbol{j}_{\rm u}$, Eq. (2). In this alternative electrochemical convention, the work flux density is defined as $\mu\boldsymbol{i}/e$, where μ is the electrochemical potential of the electron, and the heat flux density is defined as

$$\boldsymbol{q} = -\kappa\nabla T + \Pi\boldsymbol{i}. \tag{15}$$

The expressions for the divergences of these flux densities

$$\nabla\cdot\boldsymbol{q} = \nabla\cdot(-\kappa\nabla T) + \nabla\Pi\cdot\boldsymbol{i} \tag{16}$$

$$\nabla\cdot(\mu\boldsymbol{i}/e) = \boldsymbol{i}\cdot\nabla(\mu/e) = S\boldsymbol{i}\cdot\nabla T + \rho\boldsymbol{i}^2 \tag{17}$$

evidence two drawbacks: i) they involve non-measurable coefficients, such as Π and S of a single material, and ii) the electrical current density also appears in the expression of $\nabla\cdot\boldsymbol{q}$, while it should only appear in the divergence of the work flux density because it determines the electrical power. That is, although thermoelectricity involves coupled transport processes, as evidenced by Eq. (8), the description of energy transfers in terms of electrical power and heat rate is clearer when $\boldsymbol{i}$ only appears in the expression of the electrical power, as it occurs in Eq. (14). In relation to point i), note that only relative values $\Pi - \Pi_{\rm ref}$ and $S - S_{\rm ref}$ can be experimentally determined [19,21,22]. The apparent absolute values of $\Pi = TS$ and S reported in the literature consider $S_{\rm ref} = 0$.

The conclusion from the comparison of Eqs. (13) and (14), on the one hand, and Eqs. (16) and (17), on the other hand, is that the observable flux densities $\boldsymbol{j}_{\rm q}$ and $\boldsymbol{j}_{\rm w}$ in Eqs. (9) and (10) may provide a clearer description of the energy balance in the TEs.

2.3. One-dimensional description of energy transport in TEs

The work rate and the heat rate in an element (TE) of a thermoelectric device are observable quantities that can be determined from the work flux and heat flux on the boundaries of the TE, Eq. (4). In this section, work and heat fluxes at the different cross sections of a TEC (Fig. 1) are calculated. The basic unit of a TEC consists of the n-type and p-type semiconductor legs of cross section A and the copper connectors, one at cold temperature $T_{\rm c}$ and the other two at hot temperature $T_{\rm h}$. There is no heat transfer across the lateral surfaces of the legs. Under steady-state conditions the energy flux $J_{\rm u} = Aj_{\rm u}$ is constant in the semiconductor legs and the energy conservation equation, Eq. (12), is

$$\frac{\rm d}{{\rm d}x}\left(\kappa_i\frac{{\rm d}T_i}{{\rm d}x}\right) - \frac{I}{A}\tau_i\frac{{\rm d}T_i}{{\rm d}x} + \rho_i\frac{I^2}{A^2} = 0 \qquad (i = {\rm n, p}). \tag{18}$$

By integration of Eq. (18), the temperature distribution and the heat flux

$$J_{\rm q} = -\kappa A\frac{{\rm d}T}{{\rm d}x} \tag{19}$$

can be evaluated in the semiconductor legs. From $J_{\rm w} = J_{\rm q} - J_{\rm u}$, the work flux in the semiconductors is

$$J_{\rm w} = \left(\frac{\mu}{e} - \Pi\right)I. \tag{20}$$

The heat and work fluxes may be discontinuous at the connector-semiconductor junctions. These discontinuities depend on the thermal boundary conditions [23,24]. Electron-hole recombination takes place in p-type leg-hot connector junction [25] and electron-hole pair generation takes place in p-type leg-cold connector junction of a TEC. For a thermodynamic description of the energy transfers in terms of work and heat, the positions at each side of every interface must be identified. The position x_{ij} lies inside material i in contact with material j (i, j = n, p, h, c)

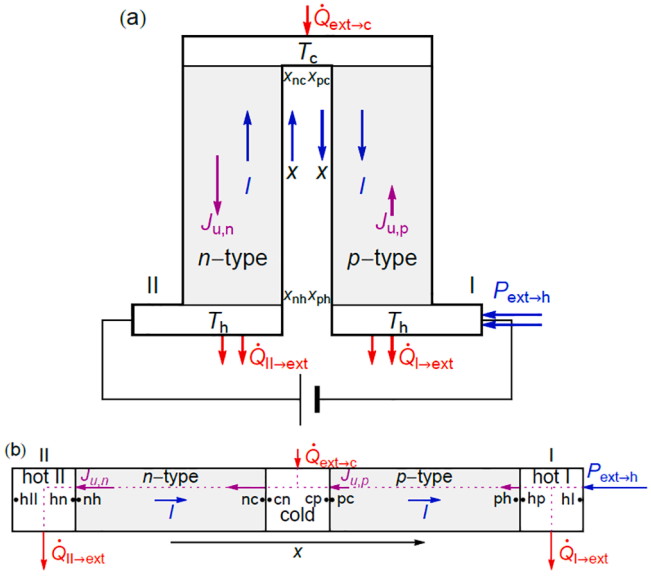

Fig. 1. (a) The basic unit of a TEC. The negative electrical terminal is marked as I, and the positive as II. (b) The energy transport can be analyzed using a coordinate x along the direction of the electric current I.

Thus, e.g., x_{nh} is a position in the n-type leg close to the junction with the hot connector (Fig. 1(b)). At these junctions, the work flux and the heat flux are deduced from the relations

$$J_{w,ji} - J_{w,ij} = \frac{1}{e}(\mu_{ji} - \mu_{ij})I - (\Pi_{ji} - \Pi_{ij})I \qquad (i = n,\ p;\ j = h,\ c) \tag{21}$$

$$J_{q,ji} = J_{q,ij} - J_{w,ij} + J_{w,ji} \qquad (i = n,\ p;\ j = h,\ c) \tag{22}$$

where $(\mu_{ji} - \mu_{ij})/e$ is determined by the contact resistance. The work flux is assumed to be constant in the connectors due to their large electrical and thermal conductivities. Thus, $J_{w,hp} = J_{w,hI}$ and $J_{w,cn} = J_{w,cp}$. As an arbitrary reference, we take $J_{w,hII} = J_{w,hn} = 0$.

3. Results and discussion

A TEC basic unit with n-type $Bi_2(Te_{0.94}Se_{0.06})_3$ and p-type $(Bi_{0.25}Sb_{0.75})_2Te_3$ legs [26–28] of cross section $A = 0.50 \times 0.50$ mm^2 and length $L = 1.0$ mm is considered. In the experimental determination of the Seebeck coefficient of n-type and p-type semiconductors using thermocouples a/b, the approximation $S_i - S_a \approx S_i - S_b \approx S_i$ (i = n, p) is invoked [20]. Consistently, we also assume $S_i - S_{connector} \approx S_i$ (i = n, p). From the reported values of the Seebeck coefficient (Table 1), the Thomson and Peltier coefficients are calculated using the Kelvin relations $\tau = T(dS/dT)$ and $\Pi = TS$. The contact resistance R_{con} of every metal–semiconductor junction is estimated as $R_{con} = (R_n + R_p)/40$, where R_n and R_p are the electrical resistances of the legs [29–32].

The steady-state heat, work and energy fluxes in the TEC basic unit (Fig. 1) have been calculated under operating conditions for $I = 1.0$ A, $T_c = 260$ K, and $T_h = 320$ K. The temperature distribution (Fig. 2) is obtained by numerical integration of Eq. (18). Following the criteria presented above, energy, heat and work fluxes have been determined (Figs. 3 and 4). Thus, we are able to evaluate the electric power received in a thermoelement from the work fluxes at its boundaries

$$P_i = -\dot{W}_i = J_{w,i,out} - J_{w,i,in} \tag{23}$$

where $J_{w,i,in}$ and $J_{w,i,out}$ are the incoming and outgoing work flux in the TE i. For example, for the n-type leg, the incoming work flux is $J_{w,nh}$ and the outgoing flux is $J_{w,nc}$ so that $P_n = -\dot{W}_n = J_{w,nc} - J_{w,nh} > 0$.

The energy flux is constant in the semiconductors (as there are no heat transfer across their lateral surfaces) and is continuous at the junctions, $J_{u,ij} = J_{u,ji}$. The heat and work fluxes are discontinuous at the junctions. The heat and work rates in the semiconductors, the connectors and the junctions (Fig. 4(c)) are calculated from Eq. (23). In the hot and cold connectors, the heat and work rate is zero: no power is supplied to these TEs. The semiconductors receive the powers $P_n = 29.8$ mW and $P_p = 28.4$ mW. They release the same amounts as heat fluxes to the junctions at their ends. The hot junctions receive the powers $P_{h|n} = 73.7$ mW and $P_{p|h} = 74.4$ mW. They release the same amounts as heat rates to the elements forming each junction (i.e., the hot connector II and the n-type semiconductor or the hot connector I and the p-type semiconductor). The cold junctions release the powers $-P_{n|c} = 54.6$ mW and $-P_{c|p} = 51.8$ mW. They receive the same amounts as heat rates from the elements forming each junction. As a whole, the TEC receives the power $P_{TEC} = 99.9$ mW and releases the same amount as heat flux to the surroundings.

Table 1
Experimental values of the transport coefficients given as second order polynomials $a\left[1 - b(T - T_0) + c(T - T_0)^2\right]$ with $T_0 = 300$ K [26–28].

	a	$10^3 b/\mathrm{K}^{-1}$	$10^6 c/\mathrm{K}^{-2}$
κ_p	1.472 Wm^{-1}K^{-1}	−1.29	13.5
κ_n	1.643 Wm^{-1}K^{-1}	−0.98	15.6
ρ_p	8.826 μΩm	5.88	8.93
ρ_n	8.239 μΩm	4.70	2.67
S_p	0.2207 mVK^{-1}	1.55	−3.15
S_n	−0.2230 mVK^{-1}	5.62	−4.65

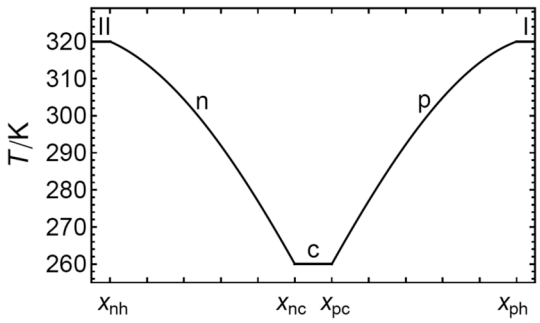

Fig. 2. Temperature distribution in the TEC for $I = 1.0$ A, $T_c = 260$ K and $T_h = 320$ K.

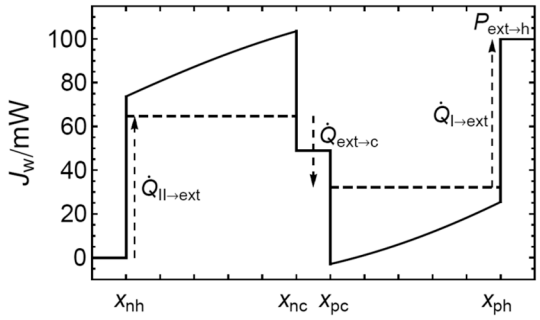

Fig. 3. Work flux J_w along the cross sections of the TEC. The dashed horizontal lines indicate the constant values of J_u in the legs. The dashed arrows show heat transfer rate with the external sources. Numerical values correspond to mW units.

We discuss next the distributions of the heat flux $Aq = \Pi I - \kappa A(dT/dx)$ and the work flux $(\mu/e)I$ in the electrochemical formalism along the elements of the TEC (Fig. 1). The relation between the heat and work fluxes in the electrochemical formalism and the heat and work fluxes in the observable formalism is

$$Aq = J_q + \Pi I \tag{24}$$

$$\frac{\mu}{e} I = J_w + \Pi I. \tag{25}$$

In the electrochemical formalism the fluxes are not measurable but they can be evaluated by the use of conventions. For example, if we assume $\Pi_c = \Pi_h = 0$ and $\Pi_{ij} = T_j S_i(T_j)$, for i = n, p and j = h, c we get the values shown in Fig. 5(a) and (b). The differences between the observable heat and work fluxes (Fig. 4(a) and (b)) and the heat and work fluxes in the electrochemical formalism are highly significant.

The heat and work rates in the TEs of the TEC can also be calculated in the electrochemical formalism. We define these rates by

$$\left[\dot{Q}\right]_i = A(q_{i,in} - q_{i,out}) \qquad (i = \mathrm{n, p, h, c, junctions}) \tag{26}$$

$$\left[\dot{W}\right]_i = \frac{1}{e}(\mu_{i,in} - \mu_{i,out})I \qquad (i = \mathrm{n, p, h, c, junctions}). \tag{27}$$

The values obtained differ significantly from the work and heat rates (compare Fig. 4(c) and 5(c)). Only when the whole TEC is considered both amounts have the same value $\left[\dot{Q}\right]_{TEC} = \left[\dot{W}\right]_{TEC} = \dot{Q}_{TEC} = \dot{W}_{TEC} = -P_{ext\to h} = -P_{TEC} = -99.9$ mW.

The use of materials with optimal values of the Thomson coefficient

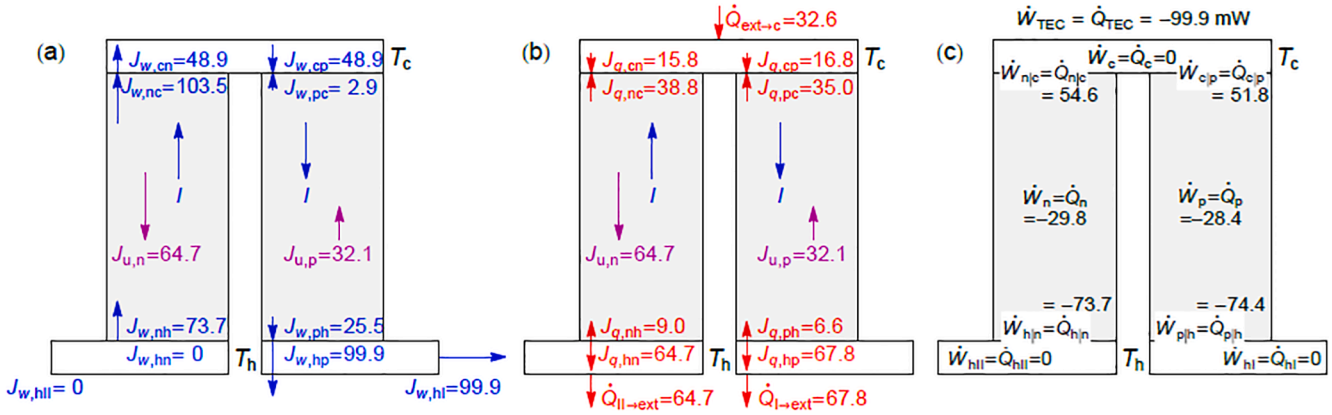

Fig. 4. Values of the observable work flux J_w (a) and the observable heat flux J_q (b) at the boundaries of the TEC elements. The energy flux J_u is constant in each leg. (c) Observable work and heat rates in the TEC and its elements. The subscript $i|j$ denotes a junction. Numerical values correspond to mW units.

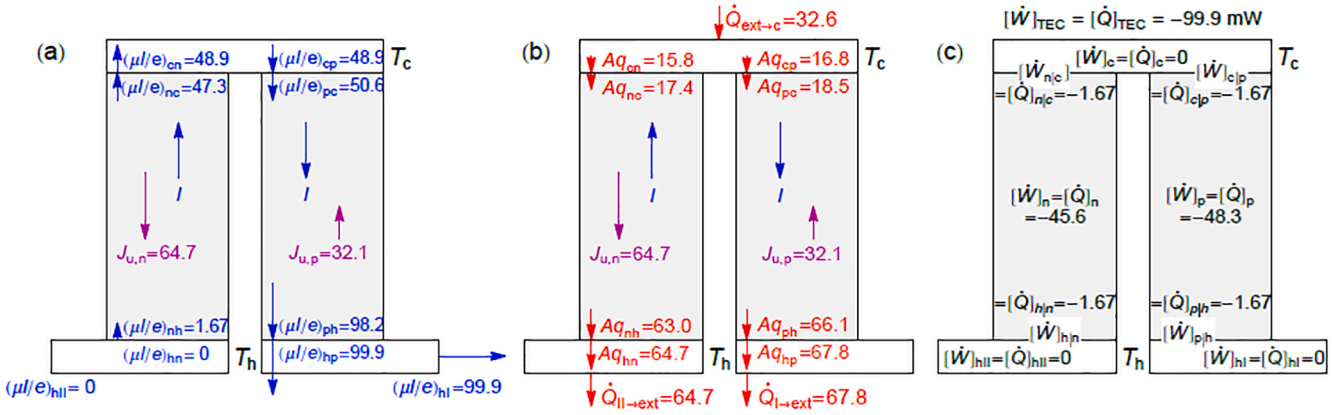

Fig. 5. Values of the fluxes $(\mu/e)I$ (a) and Aq in the electrochemical formalism (b) at the boundaries of the TEC elements. (c) Heat rate $\left[\dot{Q}\right]_i$ and work rate $\left[\dot{W}\right]_i$ in the electrochemical formalism, evaluated in the TEC and its elements. Numerical values correspond to mW units.

may improve the performance of thermoelectric coolers. Eq. (18) shows that $-\mathrm{d}J_{u,i}/\mathrm{d}x = 0$ has three contributions in the semiconductor legs: Fourier, Thomson and Joule (Fig. 6). The first is related to the gradient $\mathrm{d}J_q/\mathrm{d}x$ of the heat flux. The latter two to the gradient $\mathrm{d}J_w/\mathrm{d}x$ of the work flux. The Thomson component $-I\tau_i(\mathrm{d}T_i/\mathrm{d}x)$ may absorb a fraction of the power $\rho_i I^2/A$ that the current leaves in the semiconductor by Joule effect. In the vicinity of the cold junction, this fraction is 18% in the *n*-type leg and 33% in the *p*-type leg.

Besides the observable work and heat, the voltage is another observable in thermoelectric devices [18]. This quantity may also measure the electrical power that is consumed/generated in the TEC and in the connectors. Voltage measurement requires the use of metal Z probes [21]. The voltage distribution along the TEC (Fig. 7) can be calculated by integrating

$$\mathrm{d}V_Z = S_Z\mathrm{d}T - \mathrm{d}\left(\frac{\mu}{e}\right) = (S_Z - S)\frac{\mathrm{d}T}{\mathrm{d}x}\mathrm{d}x - \frac{\rho I}{A}\mathrm{d}x \tag{28}$$

on assuming $S_Z \approx 0$. As the power supplied to a thermoelectric element i is determined by the incoming and outgoing work fluxes

$$P_i = -\dot{W}_i = J_{w,i,\mathrm{out}} - J_{w,i,\mathrm{in}} = \left[\frac{1}{e}\left(\mu_{i,\mathrm{out}} - \mu_{i,\mathrm{in}}\right) - \left(\Pi_{i,\mathrm{out}} - \Pi_{i,\mathrm{in}}\right)\right] I \tag{29}$$

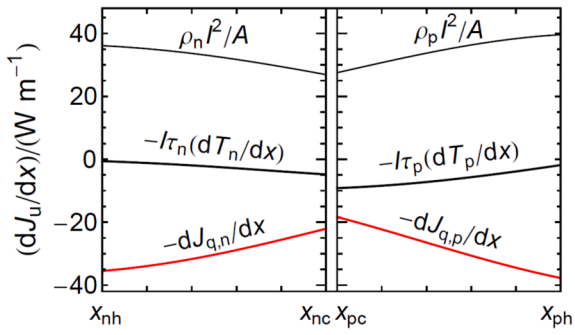

Fig. 6. Joule, Thomson and Fourier components of the energy flux gradient in the semiconductor legs. At every position x, their sum vanishes due to energy conservation. Due to the Thomson component $-I\tau_i(\mathrm{d}T_i/\mathrm{d}x)$, the current absorbs a fraction of the power dissipated due to the Joule effect.

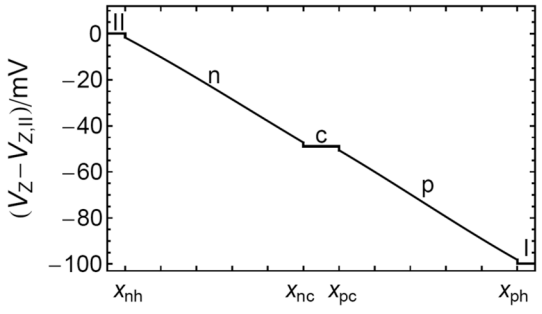

Fig. 7. The distribution of the voltage $V_Z(x) - V_{Z,II}$ in the TEC. The voltage drop at each junction is IR_{con} = 1.67 mV.

only when $\Pi_{i,\text{out}} = \Pi_{i,\text{in}}$ and $T_{i,\text{out}} = T_{i,\text{in}}$ we obtain

$$P_i = (V_{\text{Z},i,\text{in}} - V_{\text{Z},i,\text{out}})I. \tag{30}$$

Eq. (30) is only valid for the whole TEC and for the connectors, but not for the semiconductors and the junctions.

4. Conclusions

Notwithstanding that the expression $\boldsymbol{q} = -\kappa\nabla T + \Pi\boldsymbol{i}$ for the heat flux density in the electrochemical formalism may be convenient from other considerations, the observable heat flux density in thermoelectricity is $\boldsymbol{j}_\text{q} = -\kappa\nabla T$. The corresponding expression of the observable work flux density is $\boldsymbol{j}_\text{w} = (\mu/e - \Pi)\boldsymbol{i}$. That is, in order to analyze the energy flows in a TEC in terms of observable quantities, $\boldsymbol{j}_\text{q}$ and $\boldsymbol{j}_\text{w}$ are preferred to other conventional definitions. The results from the detailed analysis of the energy transfers in a basic unit of a TEC led to the conclusion that the introduction of the work flux enhances the understanding of the energy balances in the thermoelements. Since, to the best of our knowledge, no previous reference has been made to the work flux in the literature, the interpretation of thermoelectric phenomena might benefit from the introduction of the work flux.

Up to 33% of the power dissipated by the Joule effect in the semiconductors is absorbed by the Thomson effect. The voltage distribution in a TEC measures the electrical power consumed in a TEC and in its connectors, but not in the semiconductors and in the semiconductor-connector junctions.

CRediT authorship contribution statement

Javier Garrido: Conceptualization, Data curation, Investigation, Writing - original draft. **José Antonio Manzanares:** Formal analysis, Investigation, Resources, Supervision, Validation, Writing – review & editing.

Declaration of Competing Interest

The authors declare that they have no known competing financial interests or personal relationships that could have appeared to influence the work reported in this paper.

Acknowledgments

J. A. M. acknowledges the *Ministerio de Ciencia e Innovación* (Spain) and the European Regional Development Funds (FEDER), project No. PGC2018-097359-B-I00.

References

[1] H.B. Callen, The application of Onsager's reciprocal relations to thermoelectric, thermomagnetic, and galvanomagnetic effects, Phys. Rev. 73 (11) (1948) 1349–1358, https://doi.org/10.1103/PhysRev.73.1349.
[2] C.A. Domenicali, Irreversible thermodynamics of thermoelectricity, Rev. Mod. Phys. 26 (2) (1954) 237–275, https://doi.org/10.1103/RevModPhys.26.237.
[3] J.A. Manzanares, M. Jokinen, J. Cervera, On the different formalisms for the transport equations of thermoelectricity: A review, J. Non-Equilib. Thermodyn. 40 (3) (2015) 211–227, https://doi.org/10.1515/jnet-2015-0026.
[4] J. Dongxu, W. Zhongbao, J. Pou, S. Mazzoni, S. Rajoo, A. Romagnoli, Geometry optimization of thermoelectric modules: simulation and experimental study, Energy Convers. Manage. 195 (2019) 236–243, https://doi.org/10.1016/j.enconman.2019.05.003.
[5] O.V. Marchenko, Performance modeling of thermoelectric devices by perturbation method, Int. J. Therm. Sci. 129 (2018) 334–342, https://doi.org/10.1016/j.ijthermalsci.2018.03.006.
[6] C. Selvam, S. Manikandan, S.C. Kaushik, R. Lamba, S. Harish, Transient performance of a Peltier super cooler under varied electric pulse conditions with phase change material, Energy Convers. Manage. 198 (2019) 111822, https://doi.org/10.1016/j.enconman.2019.111822.
[7] Y. Apertet, C. Goupil, On the fundamental aspect of the first Kelvin's relation in thermoelectricity, Int. J. Therm. Sci. 104 (2016) 225–227, https://doi.org/10.1016/j.ijthermalsci.2016.01.009.
[8] Y. Ge, Z. Liu, H. Sun, W. Liu, Optimal design of a segmented thermoelectric generator based on three-dimensional numerical simulation and multi-objective genetic algorithm, Energy 147 (2018) 1060–1069, https://doi.org/10.1016/j.energy.2018.01.099.
[9] C. Ju, G. Dui, H.H. Zheng, L. Xin, Revisiting the temperature dependence in material properties and performance of thermoelectric materials, Energy 124 (2017) 249–257, https://doi.org/10.1016/j.energy.2017.02.020.
[10] A. Zevalkink, D.M. Smiadak, J.L. Blackburn, A.J. Ferguson, M.L. Chabinyc, O. Delaire, J. Wang, K. Kovnir, J. Martin, L.T. Schelhas, T.D. Sparks, S.D. Kang, M. T. Dylla, G.J. Snyder, B.R. Ortiz, E.S. Toberer, A practical field guide to thermoelectrics: fundamentals, synthesis, and characterization, Appl. Phys. Rev. 5 (2) (2018) 021303, https://doi.org/10.1063/1.5021094.
[11] I. Lashkevych, J.E. Velázquez, O.Y. Titov, Y.G. Gurevich, Special important aspects of the Thomson effect, J. Electr. Mater. 47 (6) (2018) 3189–3192, https://doi.org/10.1007/s11664-018-6205-x.
[12] J.L. Pérez-Aparicio, R. Palma, P. Moreno-Navarro, Elasto-thermoelectric non-linear, fully coupled, and dynamic finite element analysis of pulsed thermoelectrics, Appl. Therm. Eng. 107 (2016) 398–409, https://doi.org/10.1016/j.applthermaleng.2016.05.114.
[13] B.L. Wang, A finite element computational scheme for transient and nonlinear coupling thermoelectric fields and the associated thermal stresses in thermoelectric materials, Appl. Therm. Eng. 110 (2017) 136–143, https://doi.org/10.1016/j.applthermaleng.2016.08.115.
[14] M. Zhang, Y. Tian, H. Xie, Z. Wu, Y. Wang, Influence of Thomson effect on the thermoelectric generator, Int. J. Heat Mass Transfer 137 (2019) 1183–1190, https://doi.org/10.1016/j.ijheatmasstransfer.2019.03.155.
[15] H. Lv, X.-D. Wang, J.-H. Meng, T.-H. Wang, W.-M. Yan, Enhancement of maximum temperature drop across thermoelectric cooler through two-stage design and transient supercooling effect, Appl. Energy 175 (2016) 285–292, https://doi.org/10.1016/j.apenergy.2016.05.035.
[16] Y.G. Gurevich, G.N. Logvinov, O.Y. Titov, J. Giraldo, New physical principles of contact thermoelectric cooling, Surf. Rev. Letters 9 (2002) 1703–1708, https://doi.org/10.1142/S0218625X02004256.
[17] J. Garrido, A. Casanovas, J.A. Manzanares, Thomson power in the model constant transport coefficients for thermoelectric elements, J. Electron. Mater. 48 (9) (2019) 5821–5826, https://doi.org/10.1007/s11664-019-07351-y.
[18] J. Garrido, A. Casanovas, The central role of the Peltier coefficient in thermoelectric cooling, J. Appl. Phys. 115 (12) (2014) 123517, https://doi.org/10.1063/1.4869776.
[19] J. Garrido, Observable variables in thermoelectric phenomena, J. Phys. Chem. B 106 (41) (2002) 10722–10724, https://doi.org/10.1021/jp020196k.
[20] J. Garrido, Thermodynamics of electrochemical systems, J. Chem. Phys. B 108 (2004) 18336–18340, https://doi.org/10.1021/jp049264o.
[21] H.J. Goldsmid, Introduction to Thermoelectricity, Springer, Berlin (2010), https://doi.org/10.1007/978-3-642-00716-3.
[22] J. Garrido, Peltier's and Thomson's coefficients of thermoelectric phenomena in the observable formulation, J. Phys.: Condens. Matter 21 (15) (2009) 155802, https://doi.org/10.1088/0953-8984/21/15/155802.
[23] I. Lashkevych, Y.G. Gurevich, Boundary conditions for thermoelectric cooling in *p–n* junction, Int J Thermophys 32 (5) (2011) 1086–1097, https://doi.org/10.1007/s10765-011-0969-z.
[24] Y.G. Gurevich, I. Lashkevych, Sources of fluxes of energy, heat, and diffusion heat in a bipolar semiconductor: influence of nonequilibrium charge carriers, Int J Thermophys 34 (2) (2013) 341–349, https://doi.org/10.1007/s10765-013-1416-0.
[25] B. El Filali, O.Y. Titov, Y.G. Gurevich, Physics of charge transport in metal–monopolar (n - or p -type) semiconductor–metal structures, J. Phys. Chem. Solids 118 (2018) 14–20, https://doi.org/10.1016/j.jpcs.2018.02.047.
[26] X.-D. Wang, Y.-X. Huang, C.-H. Cheng, D. Ta-Wei Lin, C.-H. Kang, A three-dimensional numerical modeling of thermoelectric device with consideration of coupling of temperature field and electric potential field, Energy 47 (1) (2012) 488–497, https://doi.org/10.1016/j.energy.2012.09.019.
[27] J.H. Meng, X.D. Wang, X.X. Zhang, Transient modeling and dinamic characteristics of thermoelectric cooler, Appl. Energy 108 (2013) 340–348, https://doi.org/10.1016/j.apenergy.2013.03.051.
[28] O. Yamashita, S. Sugihara, High-performance bismuth-telluride compounds with highly stable thermoelectric figure of merit, J Mater Sci 40 (24) (2005) 6439–6444, https://doi.org/10.1007/s10853-005-1712-6.
[29] H.J. Goldsmid, Electronic Refrigeration, Pion, London, 1986.
[30] A. Martinez, D. Astrain, A. Rodriguez, P. Aranguren, Advanced computational model for Peltier effect based refrigerators, Appl. Therm. Eng. 95 (2016) 339–347, https://doi.org/10.1016/j.applthermaleng.2015.11.021.
[31] S.C. Kaushik, S. Manikandan, The influence of Thomson effect in the performance optimization of a two stage thermoelectric cooler, Cryogenics 72 (2015) 57–64, https://doi.org/10.1016/j.cryogenics.2015.08.004.
[32] D. Ebling, K. Bartholomé, M. Bartel, M. Jägle, Module geometry and contact resistance of thermoelectric generators analyzed by multiphysics simulation, J. Electr. Mater. 39 (9) (2010) 1376–1380, https://doi.org/10.1007/s11664-010-1331-0.